EC
Journals.ASM.org

Transcription Factor Efg1 Shows a Haploinsufficiency Phenotype in Modulating the Cell Wall Architecture and Immunogenicity of *Candida albicans*

Martin Zavrel,[a,c] Olivia Majer,[b] Karl Kuchler,[b] and Steffen Rupp[a]

Fraunhofer Institute for Interfacial Engineering and Biotechnology, Stuttgart, Germany[a]; Medical University of Vienna, Christian Doppler Laboratory for Infection Biology, Max F. Perutz Laboratories, Vienna, Austria[b]; and University of Missouri—Kansas City, School of Biological Sciences, Cell Biology and Biophysics, Kansas City, Missouri, USA[c]

The *Candida albicans* transcription factor Efg1 is known to be involved in many different cellular processes, including morphogenesis, general metabolism, and virulence. Here we show that besides its manifold roles, Efg1 also has a prominent effect on cell wall structure and composition, strongly affecting the structural glucan part. Deletion of only one allele of *EFG1* already results in severe phenotypes for cell wall biogenesis, comparable to those with deletion of both alleles, indicative of a severe haploinsufficiency for *EFG1*. The observed defects in structural setup of the cell wall, together with previously reported alterations in expression of cell surface proteins, result in altered immunogenic properties of strains with compromised Efg1 function. This is shown by interaction studies with macrophages and primary dendritic cells. The structural changes in the cell wall carbohydrate meshwork presented here, together with the manifold changes in cell wall protein composition and metabolism reported in other studies, contribute to the altered immune response mounted by innate immune cells and to the altered virulence phenotypes observed for strains lacking *EFG1*.

Many fungal pathogens, including the most prevalent human fungal pathogen, *Candida albicans*, have the ability to grow with different morphologies, as budding yeast or as filamentous invasive hyphae. The growth mode of *C. albicans* is determined by environmental conditions, including host factors. While yeast growth is favored at low temperatures and high glucose concentrations, germ tubes leading to formation of hyphae occur in the presence of various stimuli, including neutral pH, elevated CO_2 levels, higher temperatures, and the presence of serum or *N*-acetylglucosamine in the medium (2).

The transcription factor Efg1 was originally identified by its ability to promote pseudohyphal growth in the nonpathogenic yeast *Saccharomyces cerevisiae*. Efg1 is a member of the APSES family of basic helix-loop-helix transcriptional regulators and is one of the best-characterized regulators of hyphal morphogenesis in *C. albicans* (52). Efg1 is a key regulator of virulence, and like the related pseudohyphal activator Phd1 and repressor Sok2 in *S. cerevisiae*, Efg1 is regulated by the Ras-cyclic AMP (cAMP)-protein kinase A (PKA) pathway (49). Efg1 is also a key regulator of filamentation in the presence of serum (28) and is involved in the transcriptional response to it (31). Deletion of *EFG1* negatively affects filamentation under most conditions, but Efg1 acts as a filamentation repressor under oxygen limitation conditions (9, 44).

In addition to regulating the yeast-to-hypha transition, Efg1 has been implicated in numerous functions going far beyond the regulation of morphogenesis. For instance, Efg1 is required for the generation of chlamydospores (48), the white cell-specific transcriptional profile (50, 51), biofilm formation (38), regulation of cell wall proteins (9, 20, 42, 47), regulation of oxidative/fermentative metabolism (9, 20), heat stress resistance (20), and virulence (28).

Efg1 is pivotal in sensing and transmitting host signals through the cAMP-PKA signaling pathway to control chromatin modifiers such as the histone deacetylase Set3, which in turn is required for virulence (22). Interestingly, Efg1 acts as both a positive and negative regulator for different sets of target genes, and one-hybrid experiments showed that Efg1 acts primarily as a transcriptional repressor (20, 32). Numerous transcriptional profiling data demonstrate that hypha-induced genes are coregulated with genes encoding known virulence factors, including proteases and adhesins. Efg1 is directly involved in regulation of many of these genes, including *SAP4*, *SAP5*, *SAP6*, *ALS1*, *ALS3*, *HWP1*, *RBT1*, *RBT4*, *ECE1*, and many others (9, 16, 20, 43, 46, 47). The observed virulence defects after deletion of *EFG1* could be connected directly to the changed expression of cell surface proteins, such as adhesins and other virulence factors, under the control of this transcription factor (47). For example, Als3 has been shown to be crucial for binding and endocytosis of *C. albicans* by epithelia and endothelia (35).

In contrast to the congenic clinical isolate SC5314, *C. albicans* lacking Efg1 has strongly impaired adhesion and penetration of *in vitro* tissue models (8). This strain also displays reduced endocytosis and transmigration through epithelial (33, 53) or endothelial (34, 35) cells. In addition, *EFG1* null mutant cells have a lower capacity to adhere to several extracellular matrices, such as fibrinogen, fibronectin, tenascin, and laminin (42). This reduced ability to adhere to and penetrate into tissue may also result in a significantly delayed expression of human β-defensins in reconstituted human oral epithelia (30).

When *efg1/efg1* cells encounter blood, lower survival rates than those seen for the wild type (WT) are observed (13). In addition, endocytosis and killing of the *efg1/efg1* strain by polymorphonu-

Received 10 August 2011 **Accepted** 20 November 2011
Published ahead of print 2 December 2011
Address correspondence to Steffen Rupp, steffen.rupp@igb.fraunhofer.de.

doi:10.1128/EC.05206-11

TABLE 1 *C. albicans* strains used for this study

Strain	Genotype	Reference
SC5314	Wild type	19
CAI4	*ura3*::*1 imm434/ura3*::*1 imm434*	11
CAI4 URA3	*ura3*::*1 imm434/ura3*::*1 imm434 RP10*::*URA3/RP10*	This work
HLC17	*ura3*::*1 imm434/ura3*::*1 imm434 EFG1/efg1*::*hisG-URA3-hisG*	28
HLC17Rev	*ura3*::*1 imm434/ura3*::*1 imm434 EFG1/efg1*::[*EFG1p-HA-EFG1-URA3*]	This work
HLC52	*ura3*::*1 imm434/ura3*::*1 imm434 efg1*::*hisG/efg1*::*hisG-URA3-hisG*	28
HLC74	*ura3*::*1 imm434/ura3*::*1 imm434 efg1*::*hisG/efg1*::*hisG* (*EFG1*)	28

TABLE 2 Oligonucleotides used for qRT-PCR studies

Gene target	Oligonucleotides
GAPDH	CATGGCCTTCCGTGTTCCTA and GCGGCACGTCAGATCCA
IL-1β	CAACCAACAAGTGATATTCTCCATG and GATCCACACTCTCCAGCTGCA
IL-4	CATCGGCATTTTGAACGAGGTCA and CTTATCGATGAATCCAGGCATCG
IL-10	GGAAGACAATAACTGCACCCA and CCCAAGTAACCCTTAAAGTCCTG
IL-12β (p40)	GGAAGCACGGCAGCAGAATA and AACTTGAGGGAGAAGTAGGAATGG
IL-23 (p19)	GCAGATTCCAAGCCTCAGTC and TTCAACATATGCAGGTCCCA
TNF-α	CAAAATTCGAGTGACAAGCCTG and GAGATCCATGCCGTTGGC
CaEFG1	TACCACAGCACGACAAAAGC and ACTGAACTTGGGGTGATTGG
C. albicans 18S rRNA	CGATGGAAGTTTGAGGCAAT and CACGACGGAGTTTCACAAGA

clear neutrophils (PMNs) *ex vivo* occur at a higher efficiency than that for the wild-type strain. Moreover, this fungal strain causes less damage to PMNs when endocytosed (24).

Notably, loss of *EFG1* in *C. albicans* also strongly attenuates its virulence in a mouse model of systemic infection, and in combination with deletion of an additional transcription factor, Cph1, virulence is almost completely abolished (28). This effect has also been shown in other virulence models, such as the murine cornea (23), *Caenorhabditis elegans* (37), and *Drosophila melanogaster* (5), confirming severe changes in the pathophysiology of *C. albicans* in the absence of Efg1.

The fungal cell surface provides the primary contact point between the pathogen and the host, especially the host's innate immune system. As reported previously (9, 20, 47), lack of the transcription factor Efg1 leads to dramatic changes in expression of cell wall proteins such as cell wall synthesis and remodeling enzymes, including the chitinases encoded by *CHT1-3*, the chitin synthases encoded by *CHS1-5*, the β-1,3-glucan synthase subunits encoded by *FKS1*, *GSL21*, *GSC1*, and *KRE62*, the β-1,4-glucan branching enzyme encoded by *GLC3*, the β-1,6-glucan biosynthesis enzymes encoded by *KRE1* and *SKN1*, the glycosylhydrolase encoded by *CRH11*, the glycosidases encoded by *PHR1* and *SUN41*, the 1,3-β-glucanosyltransferase encoded by *PGA4*, the exo-1,3-β-glucosidase encoded by *EXG2*, the mannosyltransferase encoded by *ECM39*, and the structural protein encoded by *PIR1*. In general, most of these genes are downregulated in *efg1/efg1* cells compared to the wild type, with the strongest effect in hypha-inducing media such as alpha minimal essential medium (α-MEM) at 37°C. Nevertheless, Efg1p also has a strong impact on gene expression in yeast extract-peptone-dextrose (YPD) medium in the absence of filamentation stimuli (9, 20, 47).

The impact of these transcriptional changes on cell wall structure or polysaccharide composition in the *efg1/efg1* mutant has not been reported to date. In this report, we show that the transcription factor Efg1 strongly impacts cell wall thickness as well as its polysaccharide composition even if only one copy of the *EFG1* gene is removed. Together with the filamentation defects, this may explain the difference in *efg1/efg1* strain virulence and its impaired contact with effector cells of the innate immune system.

This new finding, in combination with other phenotypes observed previously, helps to explain the severe changes in pathophysiology of *C. albicans* devoid of *EFG1*, including the strongly altered interaction with epithelial or immune cells and reduced virulence, using mouse models of systemic infection.

MATERIALS AND METHODS

Strains and growth conditions. The *C. albicans* strains used in this study are listed in Table 1. For experiments, cells were grown to exponential phase (optical density at 600 nm [OD_{600}] of ~1.0) or post-exponential phase (OD_{600} of ~10) and cultured in rotary shakers at 30°C in YPD medium (1% yeast extract, 2% Bacto peptone, 2% glucose).

Reintroduction of *EFG1* into a heterozygous strain. A second functional allele of *EFG1* was reintroduced into the heterozygous strain HLC17 in order to complement *EFG1* haploinsufficiency. Genome excision of the *URA3* cassette in strain HLC17 was induced on SC medium containing 1 mg/ml 5-fluoroorotic acid. Selected Ura^- strains were tested for absence of the *URA3* gene by PCR (with oligonucleotides URA3_F [5′-GACCTATAGTGAGAGAGCAG-3′] and URA3_R [5′-TCTTGTCC ACCCATATCACG-3′]) and further transformed with PacI-linearized plasmid pTD38-HA (32), carrying a functional *EFG1* allele. Positive Ura^+ transformants were selected on SC agar plates without uridine. Their genomic DNAs were isolated, and Southern blotting was performed using the restriction enzyme BglII. By probing with an *EFG1* open reading frame (ORF) probe (PCR product obtained using oligonucleotides EFG1_F1 [5′-CCCCCATACCTTCCAATTCT-3′] and EFG1_R1 [5′-GAGGAGCC GAAGCAGAAGT-3′]), integration of the second functional *EFG1* allele into the originally disrupted *EFG1* locus was confirmed, thus creating HLC17Rev, containing two functional *EFG1* alleles in their original loci.

***URA3* complementation of strain CAI4.** The HindIII-restricted (for excision of the *lacZ* gene) and self-ligated plasmid pAU36RP10_KKf was used for *URA3* complementation of strain CAI4. This plasmid was previously prepared by M. Röhm by alteration of pCaEXP (4), in which the *MET3* promoter was replaced with the actin promoter (*ACT1p*) followed by the *lacZ* gene and the actin terminator (*ACT1t*). On both sides of the *lacZ* gene, HindIII sites were present and served for *lacZ* excision.

***EFG1* transcript level determination.** mRNAs from exponential-phase and post-exponential-phase YPD-grown yeast cells were isolated using an RNeasy minikit (Qiagen). Cells were disrupted by vortexing with glass beads. One microgram of mRNA was transcribed into cDNA by using a Verso cDNA synthesis kit (Thermo Scientific) following the technical bulletin of the producer. Quantitative reverse transcription-PCR (qRT-PCR) quantification of gene expression was performed in duplicate or triplicate in a LightCycler 480 instrument (Applied Biosystems), using Maxima SYBR green qPCR master mix (Fermentas) and the oligonucleotides listed in Table 2. For analysis of the data, Livak's ΔC_T method was used (27), and expression levels of Efg1 were normalized to the 18S rRNA transcript level. Results for a representative experiment based on two bi-

ological replicates are presented, with standard deviations based on qRT-PCR triplicates.

Agar plate drop tests. Drop tests were performed to test the growth phenotypes of *Candida* strains in the presence of various compounds. Yeast nitrogen base (YNB) plates containing sublethal doses of cell wall-disturbing agents were used. Agar plates without additives served as controls. In a 96-well plate, 1:10 dilution series of strains starting from an OD_{600} of 1.0 were prepared with sterile distilled water (dH_2O). Dilution series of strains were transferred from 96-well plates to agar plates by use of a 48-replica plater (Sigma-Aldrich), transferring about 4 μl of the suspension. Agar plates were incubated at 30°C for 2 days and documented by photography.

Zymolyase treatment. Cell wall Zymolyase 100T (Seikagaku) treatment was performed to investigate changes in cell wall sensitivity to the β-1,3-glucan laminarinpentaohydrolase from *Arthrobacter luteus*. The experiment was performed in 1.5-ml plastic cuvettes. YPD-grown exponential-phase or post-exponential-phase cells were pelleted, washed with dH_2O, and resuspended in dH_2O to an OD_{600} of 3.0. Approximately 400-μl aliquots of cell suspension of each strain were added to the cuvettes, together with 400 μl of 150 mM Tris-HCl, pH 7.5, containing 180 mM beta-mercaptoethanol (β-ME), and were incubated for 5 min at room temperature. Prior to measurement, 400 μl of Zymolyase 100T (concentration of 1.8 μg/ml [~0.18 U/ml] for exponential-phase cells and concentration of 30 μg/ml [~3 U/ml] for post-exponential-phase cells [OD, ~10]) in dH_2O was added; the OD_{600} in cuvettes was read every 5 min over a 1-h period. The content of the cuvettes was resuspended by vortex mixing prior to each measurement.

Electron microscopy. Two milliliters of exponentially growing *Candida* cells in YPD (OD_{600}, ~1.0) was fixed for 1 h at 4°C with 2.5% glutaraldehyde. After fixation, cells were washed three times for 15 min each with 1 ml of fresh YPD. After the last wash, 0.5 ml 2% $KMnO_4$ in dH_2O was added to the cells and incubated at room temperature for 90 min. Cells were washed three times with 1 ml dH_2O and then slowly dehydrated by incubation with 1 ml each of 30%, 50%, 70%, 90%, and 100% acetone for 15 min each, with centrifugation after each step (1 min, 2,000 $\times$ *g*). Finally, cells were washed twice in absolute acetone and incubated for 1 h in a mixture of 1/3 Spurr's medium-hard resin (Polysciences) and 2/3 acetone in a closed Eppendorf tube. Tubes were then opened, and the acetone was evaporated overnight at room temperature. The cells were incubated twice for 1 h with fresh Spurr's resin, overlaid by the resin in 5.6-mm Beem capsules, and baked at 65°C for 48 h. After trimming with a razor blade, samples were sectioned with glass knives to 70-nm sections (Ultramicrotom; Leica Ultracut) and collected on a water surface. Sections were transferred to the surface of mesh grids covered with Pioloform support film and stained for 6 min in 1% uranyl acetate and, after washing with dH_2O for an additional 4 min, in 1% lead citrate. Washed and dried samples were examined and documented using an electron microscope (FEI Tecnai G2 microscope equipped with a Tietz F224 digital camera). Multiple cells of each strain were imaged. The average cell wall thickness, from the membrane to the middle of the electron-dense outer mannoprotein layer, was measured manually for at least 20 individual yeast cells.

Cell wall isolation and determination of polysaccharide composition. Briefly, 50 to 100 ml of exponential-phase or post-exponential-phase cells in YPD medium was washed twice with dH_2O. Cells were resuspended in 1 ml of 10 mM Tris-HCl, pH 7.5, and kept on ice. To the suspension, 300 μl of glass beads was added (0.25- to 0.5-mm diameter; Roth), and the sample was intensively vortex mixed at 4°C for 30 min. The disrupted cell suspension was recovered and washed twice with 1 ml of dH_2O. Cell walls were extracted three times at 100°C with 1 ml of extraction buffer (50 mM Tris-HCl, pH 7.8, 2% SDS, 10 mM EDTA, 40 mM β-mercaptoethanol). The pellet was washed five times with 1 ml dH_2O, frozen, and then lyophilized.

The hydrolysis protocol was modified from a previously described method (14). About 10 mg of lyophilized cell walls was incubated in 1.5-ml Eppendorf tubes with 75 μl of 72% H_2SO_4 for 3 h at room temperature. After 3 h, 950 μl of dH_2O containing 1 mg/ml galactose was added as an internal control. Reaction tubes were incubated for another 4 h at 100°C. The mixtures were then transferred to 15-ml Falcon tubes. Reaction tubes were rinsed twice with 1 ml dH_2O, and this was collected in the Falcon tubes as well. The acid solution was neutralized with about 4 ml of saturated $Ba(OH)_2$ water solution (approximately 40 g/liter). The precipitate was left to be formed overnight at 4°C. The pH was then adjusted to between 6.0 and 8.0 [with H_2SO_4 and $Ba(OH)_2$], and the final volume was adjusted to 10 ml with dH_2O. The formed precipitate was centrifuged and discarded. Finally, the sugar content was determined by high-performance ion chromatography (HPIC) measurement (using glucosamine for chitin, glucose for β-1,3- and β-1,6-glucans, mannose for mannans, and galactose as an internal control), using standard dilutions for calibration.

To determine the absolute amount of glucose relative to cell biomass, 50 ml of exponential-phase or post-exponential-phase cells in YPD medium was pelleted and washed twice with dH_2O. The cell pellet was frozen and lyophilized. Approximately 10-mg specimens (the exact weight was recorded) of lyophilized cells were resuspended in 1.5-ml Eppendorf tubes in 75 μl of dH_2O. Additionally, 75 μl of 72% H_2SO_4 was added, and the samples were incubated for 3 h at 60°C. After 3 h, 850 μl of dH_2O was added, and reaction tubes were transferred for another 4 h to a heating block set at 100°C. After hydrolysis, the glucose concentration was determined using an enzyme-coupled reaction (29). The total amount of glucose was related to the biomass used for hydrolysis. This enzymatic reaction has a high specificity for glucose and is unaffected by other monosaccharides.

For measurements of intracellular glucose units, about 10 mg of dry cell biomass was disrupted in 1 ml of dH_2O with 300 μl glass beads by vortex mixing at 4°C for 30 min. To hydrate all of the polysaccharides, samples were incubated at 100°C for 15 min and then shortly vortex mixed. The glass beads and the solid parts of the cells were spun down. To 500 μl of the suspension, 50 μl of 72% H_2SO_4 was added, and the suspension was incubated at 100°C for 6 h. After hydrolysis, glucose concentrations were measured as described above, and concentrations were related to the cell biomass used for glass bead disruption.

β-1,3-Glucan staining and analysis. Approximately 1×10^8 *Candida* cells were fixed for 5 min in 3.7% formaldehyde, washed with phosphate-buffered saline (PBS), and blocked for 1 h with 1 ml PBS plus 2% bovine serum albumin (BSA) at room temperature with rotation. Cells were stained with mouse anti-β-1,3-glucan primary antibody (100 μl [1:100] in PBS plus 2% BSA; original antibody concentration, 1 mg/ml; Biosupplies) for 1 h with rotation at room temperature. Cells were washed four times with 1 ml of PBS. Secondary antibody staining was performed for 1 h with rotation at room temperature with Alexa 488-conjugated goat anti-mouse antibody (1:100 in 100 μl PBS plus 2% BSA; Invitrogen). During this step, samples were protected from light. Cells were washed 4 times with 1 ml PBS. Unstained cells and cells stained only with the secondary antibody were used as negative controls. Cells were examined microscopically using an Axiovert 200 M microscope (Zeiss) with an appropriate fluorescence filter and a constant exposition time for all samples. Pictures were further processed using Adobe Photoshop, keeping the original size ratio and color intensity. The intensity of the fluorescence signal was measured with Aida software, using one-dimensional densitometry. Fluorescence intensity and particle size were additionally quantified using a Beckman Coulter Epics XL/MCL flow cytometer with excitation at 488 nm and emission at 525 $\pm$ 10 nm. Collected data were analyzed using FlowJo software. Intensities and cell sizes are presented as averages for three biological replicates, with standard deviations.

Reactive oxygen species (ROS) assay using the RAW264.7 macrophage cell line. The murine macrophage RAW264.7 cell line (ATCC TIB-71) (39) was grown in supplemented Dulbecco's modified Eagle's medium (DMEM; 10% fetal calf serum [FCS], 0.075% $NaHCO_3$, 1 mM sodium pyruvate, 0.1 mg/ml gentamicin) at 37°C with 5% CO_2. When grown to confluence, macrophages were detached from the 75-cm^2 cell culture flask

(Greiner) by using trypsin-EDTA (Gibco). For chemiluminescence assay, the RAW264.7 cells were harvested using a cell scraper, further resuspended in HEPES-buffered BSA (10 mM HEPES, pH 7.3, 5.5 mM glucose, 1 mM $MgCl_2$, 5 mM KCl, 145 mM NaCl, 4 mM $NaHCO_3$, 1 mM $CaCl_2$, 0.1% BSA, pH 7.3), and diluted to 2×10^6 cells/ml. From this suspension, 50 μl (1×10^5 cells) per well was added to a white 96-well plate (Nunc). After incubation at 37°C and 5% CO_2 in the dark for about 30 min, 100 μl of HEPES-buffered BSA containing 0.2 mM luminol (Sigma) and 40 U/ml horseradish peroxidase (HRP) type VI (Sigma) was added. Prior to measurement, either 50 μl of HEPES-buffered BSA containing unopsonized zymosan (100 μg/ml; Sigma) or 5×10^5 *Candida* cells (1×10^7 cells/ml) were added to the wells. HEPES-buffered BSA served as a negative control. The well content was mixed thoroughly. Chemiluminescence emitted from each well was immediately recorded in the dark at 37°C for 120 min at 2.5-min intervals in a 96-well plate reader (Synergy 2; BioTek). Luminescence is given in relative luminescence units (RLU) s^{-1}.

Interaction of *Candida* cells with mDCs. Bone marrow-derived murine (from 7- to 9-week-old C57BL/6 wild-type mice) myeloid dendritic cells (mDCs) were obtained exactly as described earlier (15), and differentiated cells were plated in 30-mm plates (1×10^6 mDCs/dish; 3 ml). The next day, cells from exponentially growing *Candida* cultures (in YPD) were pelleted and resuspended in PBS. After estimations of cell counts, dendritic cells were infected with 100 μl of *Candida* cell suspension (2×10^7 cells/ml) at a multiplicity of infection (MOI) of 2:1 (*Candida* cells:mDCs) and were incubated at 37°C and 5% CO_2. After 4 h of incubation, plates were placed on ice and the medium was aspirated (except for the negative control, where mDCs in medium were nonadhered). The medium from negative controls was centrifuged, and 175 μl of RNA lysis buffer (Promega) containing β-ME was added to the pellet. To the infected plates, 175 μl of the same buffer was added, and mDCs were scraped off the plates. Samples were placed on filter columns (Macherey-Nagel), and DNA was sheared by centrifugation. Supernatants from the flowthrough were collected, and RNA was extracted using an SV total RNA isolation system (Promega) according to the manufacturer's instructions. About 1 μg of RNA was transcribed into cDNA by using a reverse transcription system (Promega) following the technical bulletin of the producer. qRT-PCR quantification of gene expression was performed in a Mastercycler EP Realplex system (Eppendorf), using Mesa green qPCR MasterMix Plus for SYBR green assay (Eurogentec), along with the oligonucleotides listed in Table 2. For analysis of the data, Livak's ΔC_T method was used (27), and expression levels of cytokines were normalized to the glyceraldehyde-3-phosphate dehydrogenase (GAPDH) transcript level. Results for a representative experiment based on two biological replicates are presented, with standard deviations based on qRT-PCR triplicates.

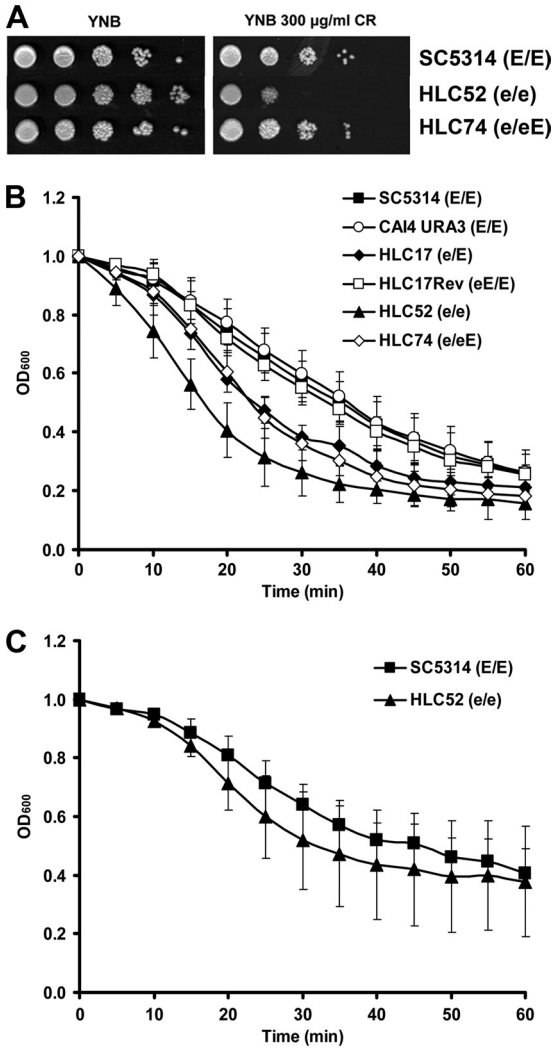

FIG 1 (A) Drop tests for sensitivity to the cell wall-disturbing agent Congo red (CR). Plates were cultivated at 30°C and documented after 2 days. The sensitivities of post-exponential-phase (B) and exponentially growing (C) cells to Zymolyase 100T are shown. Data represent averages for three independent experiments.

RESULTS

Deletion of *EFG1* affects structural components in the *C. albicans* cell wall. Efg1 is a central regulator of gene expression, including that of genes that encode cell wall remodeling enzymes (9, 20, 47). However, until now, consequences of *EFG1* deletion on cell wall structures have not been described, and only a few biochemical data are available concerning changes in protein and carbohydrate composition. Previous experiments showed that a strain lacking *EFG1* is hypersensitive to calcofluor white (20), which acts on the chitin layer, indicating impaired cell wall biogenesis. In contrast, Congo red is considered to act on the cell wall glucan structure (21, 40). In agar plate assays, an *efg1/efg1* null mutant (HLC52) showed a high sensitivity to Congo red which was restored to WT levels in a revertant strain harboring a restored functional allele of *EFG1* (HLC74) (Fig. 1A). This result indicates that the glucan structure in an *EFG1* deletion strain is also perturbed.

To further confirm the apparent cell wall defects, we incubated exponentially growing cells of SC5314 and HLC52 (*efg1/efg1*) with Zymolyase 100T. Zymolyase hydrolyzes β-1,3-glucan and thereby destroys the cell wall. Thus, the kinetics of Zymolyase digestion may reflect changes in cell wall structure, predominantly in its glucan component. By analyzing exponentially growing cells, no statistically significant differences between the wild type and the HLC52 *efg1/efg1* null mutant were detectable (Fig. 1C), consistent with previous work (20). Using cells from post-exponential-phase cultures (OD, ~10), however, we observed a significantly increased sensitivity of the *EFG1* deletion strain (HLC52) compared to the wild type (Fig. 1B). For the *EFG1*-reconstituted strain (HLC74), we observed only a partial reversion of the phenotype to one somewhere between those of the wild type and the null mutant, indicating an *EFG1* gene dosage effect. Similar kinetics of degradation were observed for the *efg1/EFG1* heterozygous strain (HLC17). Reversion of the heterozygote by reintegration of a second functional *EFG1* allele (HLC17Rev) at the genomic *EFG1* locus resulted in full reversion of the phenotype and in kinetics of degradation identical to those of wild-type strain SC5314, confirming the observed gene dosage effect for *EFG1*. In addition,

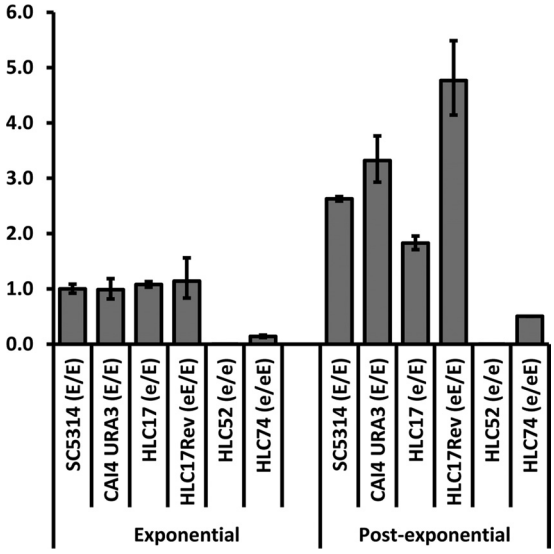

FIG 2 Transcriptional analysis of *EFG1*. Levels of *EFG1* mRNA transcripts were determined for exponential-phase and post-exponential-phase cells of strains carrying one or two copies of *EFG1*. Levels were normalized to the 18S rRNA transcript level. In total, three biological replicates were performed, and the results of a representative one are presented, with standard errors originating from qRT-PCR replicates. For each strain, mRNA levels were related to the absolute level of *EFG1* transcripts in exponentially growing wild-type SC5314, which was set to 1.

strain CAI4 URA3, a newly prepared *URA3* revertant of the *ura3/ura3* auxotrophic strain CAI4 (11), was included in the assay in order to exclude a *URA3* positioning effect. As expected, this strain displayed cell wall properties similar to those of wild-type strain SC5314 in this assay.

These data show that deletion of the *EFG1* gene not only has a prominent effect on the cell wall protein composition, as reported previously (47), but most likely also has an effect on the polysaccharide matrix. Interestingly, the stronger effect in aging cells implies a crucial role of Efg1 in cell wall homeostasis during post-exponential-phase growth.

Transcriptional analysis of *EFG1* mRNA levels. In order to verify if the gene copy number is actually reflected in the transcript level of *EFG1*, its mRNA levels in exponential-phase and post-exponential-phase strains were measured using quantitative real-time PCR (Fig. 2). 18S rRNA was used for normalization, since the expression levels of two other genes tested for this purpose (*ACT1* and *TDH3*) were affected by the different conditions used (exponential-phase versus post-exponential-phase growth). In total, three biological replicates were performed. We observed a measurable degree of variation among the three biological replicates, most likely due to the low level of *EFG1* transcripts. Nevertheless, for all experiments, we saw no *EFG1* transcript for the HLC52 deletion mutant and significantly lower transcript levels for the HLC74 revertant, not reaching the levels in the heterozygote strain HLC17, during both exponential- and post-exponential-phase growth. The heterozygote (HLC17) and heterozygote revertant (HLC17Rev) strain displayed the most variation. However, as shown in Fig. 2, especially for post-exponential-phase cells, *EFG1* transcript levels in general were higher in HLC17Rev than in SC5314, whereas they were lower in HLC17. In exponentially growing cells, only HLC74 showed consistently lower levels of *EFG1* transcript than the WT, whereas the measurements in the other strains did not reveal significant differences within the error rate of the experiment. This confirmed, at least for post-exponential-phase cells, a gene dose- and, to a certain extent, allele-specific effect. An interesting additional result was the increase in *EFG1* expression during post-exponential-phase growth, which actually enabled detection of the differences in the respective strains. This was also reflected in the differences in Zymolyase sensitivity between exponential-phase and post-exponential-phase cells, as described above.

Deletion of *EFG1* affects cell wall polysaccharide composition and the internal carbohydrate pool. To analyze the impact of *EFG1* on the structure of the cell wall, we determined the cell surface polysaccharide composition in strains with different copy numbers of *EFG1* expressed from two different genomic loci (Fig. 3). First, the total release of glucose units by acid hydrolysis of dry cell biomass was determined for both exponential-phase and post-exponential-phase strains, using an enzyme-coupled reaction specific for glucose. The most abundant polysaccharides in the cell wall are β-1,3- and β-1,6-glucans, which are converted to glucose units. To account for glucose-containing carbohydrates present in the cytosol (mainly trehalose and glycogen), cells were lysed by disruption with glass beads. After separation of the cell wall fragments by centrifugation, the glucose concentration was determined following acid hydrolysis of total cell extracts (Fig. 3A).

Although the copy number and position of the *URA3* gene in strain CAI4 URA3 did not seem to have any effect, deletion of *EFG1* had a significant effect on both glucose pools in the cell (stored in the form of trehalose and glycogen) and the glucans of the cell wall in exponential-phase and post-exponential-phase cells. Determination of the entire amount of glucose released from the different strains showed that deletion of *EFG1* resulted in a reduction of 33% compared to the WT level. For cell wall carbohydrates, a reduction of 16% was determined, whereas internal glucose pools were reduced by almost 60% in an *efg1/efg1* null mutant (HLC52). Reconstitution of one allele of *EFG1* from the *LEU2* locus (HLC74) did not result in full reversion of this phenotype to the WT level. This is consistent with the phenotype of the initial heterozygous strain (HLC17). The total, cell wall-bound, and internal glucose pools were reduced by 14%, 10%, and 40%, respectively, for the heterozygote HLC17 and by 12%, 6%, and 40%, respectively, for the revertant strain HLC74. However, reintegration of a second allele of *EFG1* in HLC17 (*efg1/EFG1*), generating strain HLC17rev, which again contained two copies of *EFG1* at the original genomic loci, restored the levels of all glucose pools analyzed to WT levels. No statistically significant differences in glucose levels related to biomass (both cell wall related and intracellular) were observed between exponential-phase and post-exponential-phase cells in this case (Fig. 3A and data not shown).

These results indicate that deletion of even one *EFG1* allele is crucial for the level of intracellular, cell wall, and, consequently, total glucose pools in *C. albicans*. Our results reflect a strong haploinsufficiency phenotype of *EFG1* for cell wall biogenesis and maintenance of cellular glucose pools. The significant differences in glucose and glucan contents in the strains investigated may be explained by an altered metabolism, as reported previously for an *efg1/efg1* null mutant strain (9, 20). Deletion of *EFG1* enhances oxidative metabolism, while genes required for glycolysis and glu-

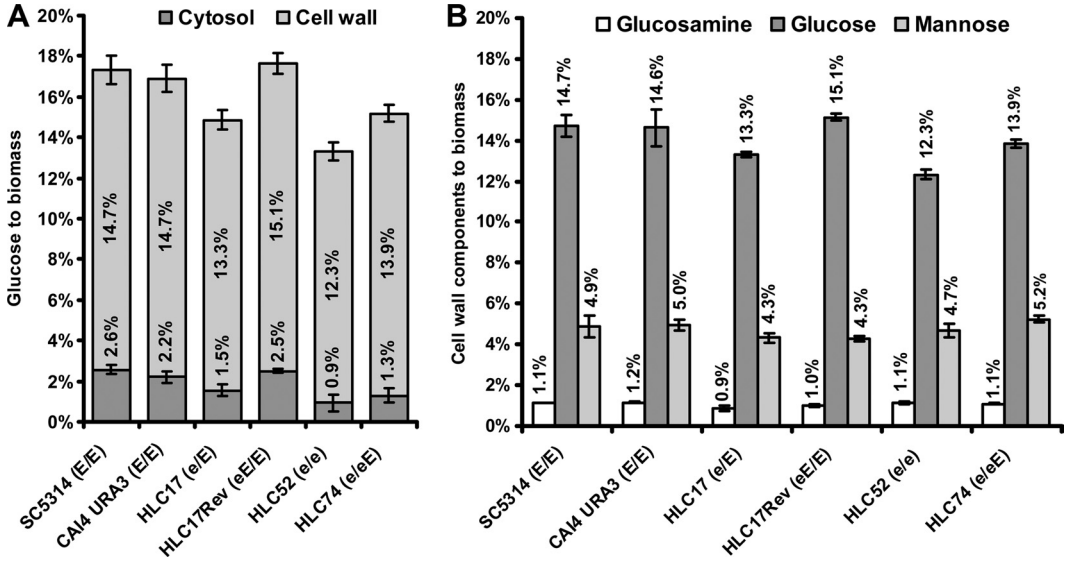

FIG 3 Polysaccharide composition of the fungal cell wall. (A) Absolute amounts of glucose released by hydrolysis of total dry cell biomass and cytosolic contents of exponentially growing strains SC5314, CAI4 URA3, HLC17, HLC17Rev, HLC52, and HLC74. (B) Absolute polysaccharide cell wall compositions related to dry cell biomass of exponentially growing strains. All of the data are based on three independent experiments, and average values with standard deviations are presented.

coneogenesis are repressed. This is expected to result in reduced glucose pools in the cell.

In addition to the ratio of glucan-bound glucose units to the dry cell biomass, the ratios of glucose (glucans), glucosamine (chitin), and mannose (mannosylated proteins) were determined by HPIC after acid hydrolysis of purified cell walls. Their relative amounts are listed in Table 3. By correlating the proportions of the individual sugars to the absolute amount of cell wall glucose related to the dry cell biomass, we were able to determine the absolute amounts of the individual cell wall components. Using this approach, we could determine which components in the cell wall remained constant and which components changed (Fig. 3B). As shown in Fig. 3A, the decrease of glucan levels of about 16% in the *efg1/efg1* strain (HLC52) was close to the number for the strains containing only one *EFG1* allele, while strain CAI4 URA3 was consistent in cell wall composition with wild-type strain SC5314, excluding a position effect of *URA3* as the cause for this result. On the other hand, we could not detect significant differences in the chitin levels of all strains tested. Although the mannan levels did show differences among the strains, no significance with regard to the copy number of *EFG1* could be observed. This indicates that *EFG1* has its strongest impact on the biosynthesis of the glucan meshwork and seems to have only a minor impact on chitin biosynthesis. The total amount of cell wall polysaccharide components for the wild-type strain SC5314 was determined to be 21.4% of the total cell mass in exponentially growing cells. This is in agreement with previous findings showing that the cell wall mass represents about one-fifth of the total cell biomass and validates the general proceedings of these experiments. Again, post-exponential-phase cells showed no significant changes in relative cell wall composition compared to exponentially growing cells (data not shown).

TABLE 3 Relative cell wall compositions of different strains

Strain[a]	% of component (mean ± SD)		
	Glucans	Mannans	Chitin
SC5314 (*EFG1/EFG1*)	71.0 ± 2.5	23.5 ± 2.6	5.5 ± 0.1
CAI4 URA3 (*EFG1/EFG1*)	70.5 ± 4.3	23.9 ± 1.4	5.6 ± 0.0
HLC17 (*efg1/EFG1*)	71.9 ± 0.8	23.4 ± 1.3	4.7 ± 0.6
HLC17Rev (eE/*EFG1*)	74.1 ± 0.8	20.1 ± 0.8	4.9 ± 0.2
HLC52 (*efg1/efg1*)	68.0 ± 1.2	25.8 ± 1.7	6.2 ± 0.4
HLC74 (*efg1*/eE)	68.6 ± 1.0	26.0 ± 0.8	5.5 ± 0.2

[a] eE, the *efg1* allele was complemented with the *EFG1* gene.

Deletion of *EFG1* reduces cell wall thickness. The total amount of cell wall polysaccharides was reduced by about 20% in HLC52 compared to the wild-type strain SC5314. This should have a severe impact on the cell wall thickness and/or structure. To investigate changes in the physical dimensions, we analyzed cell wall morphology by using transmission electron microscopy. Interestingly, the average thickness of the cell wall of the *efg1/efg1* strain (HLC52) was reduced to only 57% of the width of the wild-type cell wall (Fig. 4). The average thickness of the SC5314 cell wall in electron microscopy images was 82.7 ± 7.8 nm, while the thickness of the *efg1/efg1* cell wall was 47.1 ± 6.8 nm. Although these data are somewhat artificial due to cell fixation for electron microscopy and thus may not directly reflect the *in vivo* situation, the relative changes in cell wall thickness among strains allow them to be compared with each other. In strains containing only one functional allele of *EFG1* (heterozygote strain HLC17 and revertant strain HLC74), we observed an average reduction of about 15% from the wild-type thickness, but individual cells of SC5314, HLC17, and HLC74 showed overlapping cell wall thicknesses. Reintroduction of the second allele into the heterozygous strain (HLC17Rev) resulted in the same average cell wall thickness as that of wild-type strain SC5314. On the other hand, in CAI4 URA3, the cell wall thickness remained unaltered from that of wild-type strain SC5314. This further supports the hypothesis that the cell wall effects are dependent on *EFG1* rather than on *URA3*'s position and copy number in the respective strains. These data are

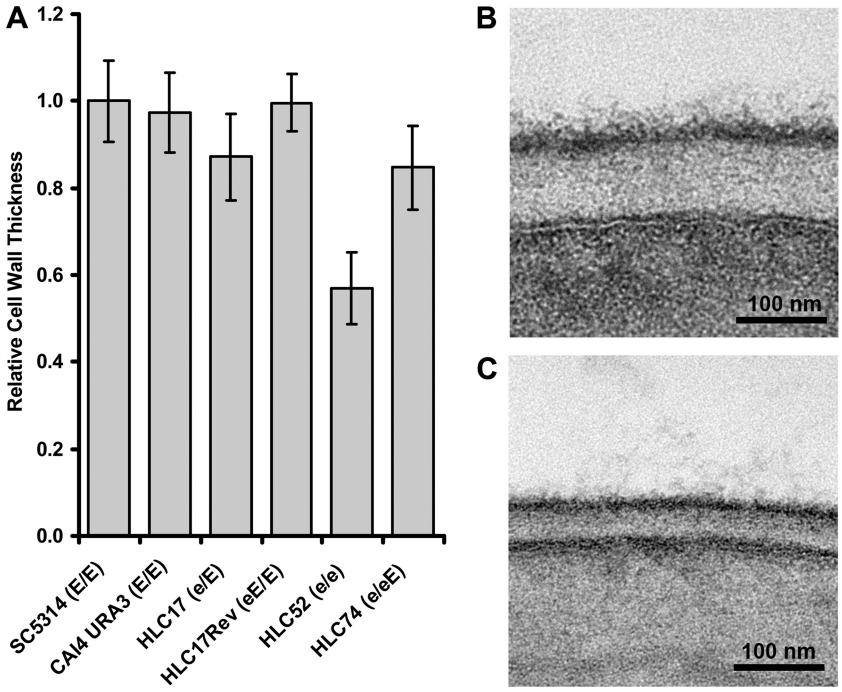

FIG 4 Cell wall thicknesses and representative transmission electron microscopy images. (A) Cell wall thicknesses were estimated from over 20 independent cell measurements obtained from different microscopic images. Representative images of the cell walls of wild-type strain SC5314 (B) and the *efg1/efg1* mutant HLC52 (C) present differences in thickness of the electron-translucent polysaccharide layer. Images were taken at a magnification of ×20,000 and represent identical areas.

also consistent with the reduced amounts of carbohydrates found in strains lacking at least one copy of the *EFG1* gene. This additionally supports our results showing that deletion of one *EFG1* gene copy in the *C. albicans* genome already has a prominent effect on the cell wall structure, most likely due to reduced glucose pools in such strains. Apart from the β-glucan layer thickness, all strains had similar cell wall architectures, consisting of an electron-dense outer layer, assigned to mannoproteins, and an electron-lucent inner layer, assigned to β-glucans and chitin.

***EFG1* affects β-1,3-glucan exposure.** To check if the structural changes in the cell wall also have consequences on β-glucan exposure, which is considered a critical virulence factor in *C. albicans* (54), we visualized β-glucan in exponentially growing cells of the respective strains (SC5314, CAI4 URA3, HLC17, HLC17Rev, HLC52, and HLC74) by using a β-1,3-glucan-specific antibody (Fig. 5A). Interestingly, immunodecoration of these strains indicated a clear difference already after deletion of one *EFG1* allele compared to the WT. When the data were quantified by fluorescence-activated cell sorter (FACS) analysis (Fig. 5B), exponential-phase and post-exponential-phase cells of strains HLC17, HLC17Rev, HLC52, and HLC74 displayed significantly higher signals, with at least 2-fold increases in intensity, than the wild type. However, strain HLC52, with both *EFG1* alleles deleted, showed a slightly smaller increase in β-1,3-glucan exposure than strains HLC17, HLC17Rev, and HLC74 (80% for exponential-phase cells and 25% for post-exponential-phase cells). The *URA3*-complemented CAI4 strain displayed fluorescence signal intensities comparable to those of the wild type. In general, post-exponential-phase cells attracted significantly smaller amounts of bound β-1,3-glucan antibodies, but we observed similar relationships between the strains analyzed to those for exponentially grown cells (Fig. 5B).

Interaction with macrophages and ROS release. The production of ROS by innate immune cells is part of the first line of defense against pathogens (6, 12). ROS assays can thus be used to evaluate recognition of microbes by the immune system (18). Although the molecular identities of ligands triggering the ROS response are not fully characterized, the main candidates include β-1,3- and β-1,6-glucans (17, 41). The changed β-1,3-glucan exposure and general changes in cell wall architecture in the *efg1/efg1* strain (HLC52) implied a high probability of altered immunological properties of HLC52. Therefore, we employed the murine macrophage cell line RAW264.7 to analyze the release of ROS during contact with our fungal strains (Fig. 6). Zymosan, a crude cell wall preparation from *Saccharomyces cerevisiae*, served as a positive control for triggering the ROS response. In the assay, we employed exponential-phase (OD_{600}, ~1) and post-exponential-phase (OD_{600}, ~10) cells to check the immunogenic properties of fungal strains in distinct growth phases.

For SC5314 and CAI4 URA3, we observed rapidly induced ROS levels upon incubation with macrophages (Fig. 6A and B). Most interestingly, the growth phase of both strains strongly modulated the intensity of ROS release of macrophages. Post-exponential-phase cells showed 6- to 7-fold-increased ROS levels compared to exponentially growing cells, although the ROS release was slightly delayed. Exponentially growing *efg1/efg1* cells also triggered significant ROS release, with a short delay in induction similar to the delay for post-exponential-phase SC5314 or CAI4 URA3 cells. When exponentially growing strains with one functional *EFG1* copy (heterozygote strain HLC17 and revertant

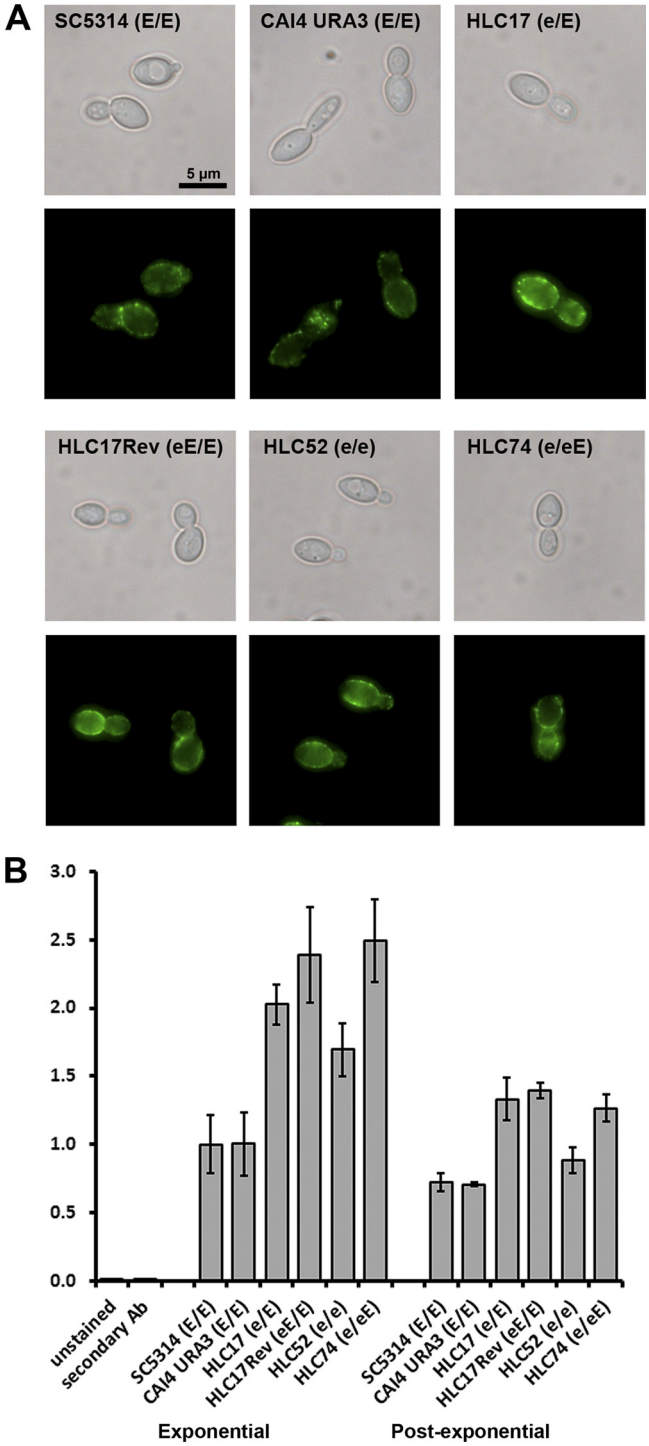

FIG 5 β-1,3-Glucan antibody staining of the cell surface. (A) Exponentially growing and β-1,3-glucan antibody-labeled strains were examined under a microscope. All figures represent equal areas. Fluorescent images were taken with a constant exposition time to compare signal intensities. For control samples labeled only with secondary antibodies, no visible fluorescence was detectable (not shown). (B) Labeled β-1,3-glucan in exponential-phase and post-exponential-phase cells was quantified by FACS analysis. Intensity medians for three biological replicates were combined and supplemented with standard errors. Fluorescence intensity was normalized to that of exponentially grown wild-type SC5314, which was set to 1.

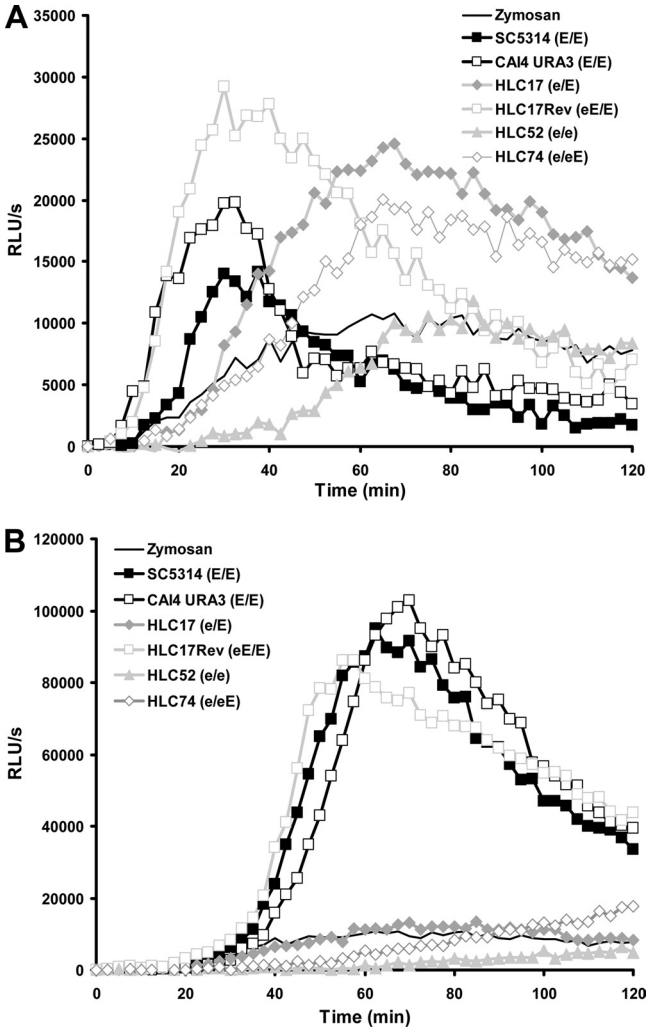

FIG 6 ROS release by macrophages challenged with strains SC5314, CAI4 URA3, HLC17, HLC17Rev, HLC52, and HLC74 in exponential-phase (A) or post-exponential-phase (B) growth. Data were reproduced in three independent experiments performed in quadruplicate. Average results for representative experiments are presented. Standard deviations for individual time points were within 10% of absolute values.

strain HLC74) were examined, they showed the same delay in ROS release as the *efg1/efg1* strain (HLC52). ROS levels exceeded the WT level by 30% to 60% but were in the range of the CAI4 URA3 levels. HLC17Rev, containing two copies of *EFG1*, also displayed an ROS response under these conditions, with the same kinetics as the wild type, although at up to 2-fold higher levels (up to 1.5-fold higher than CAI4 URA3 levels). CAI4 URA3 displayed similar kinetics to wild-type strain SC5314 and HLC17Rev, both containing two *EFG1* copies, with intensities between those of SC5314 and HLC17Rev.

During post-exponential-phase growth, SC5314, CAI4 URA3, and HLC17Rev showed highly similar ROS responses, both in strength and in the time point of induction. However, under these conditions, a severe reduction in ROS response in strains lacking one or two copies of *EFG1* was apparent, by a factor of 10 or more. In fact, the ROS levels in these strains remained more or less at the levels in exponentially growing strains. Thus, we did not see an

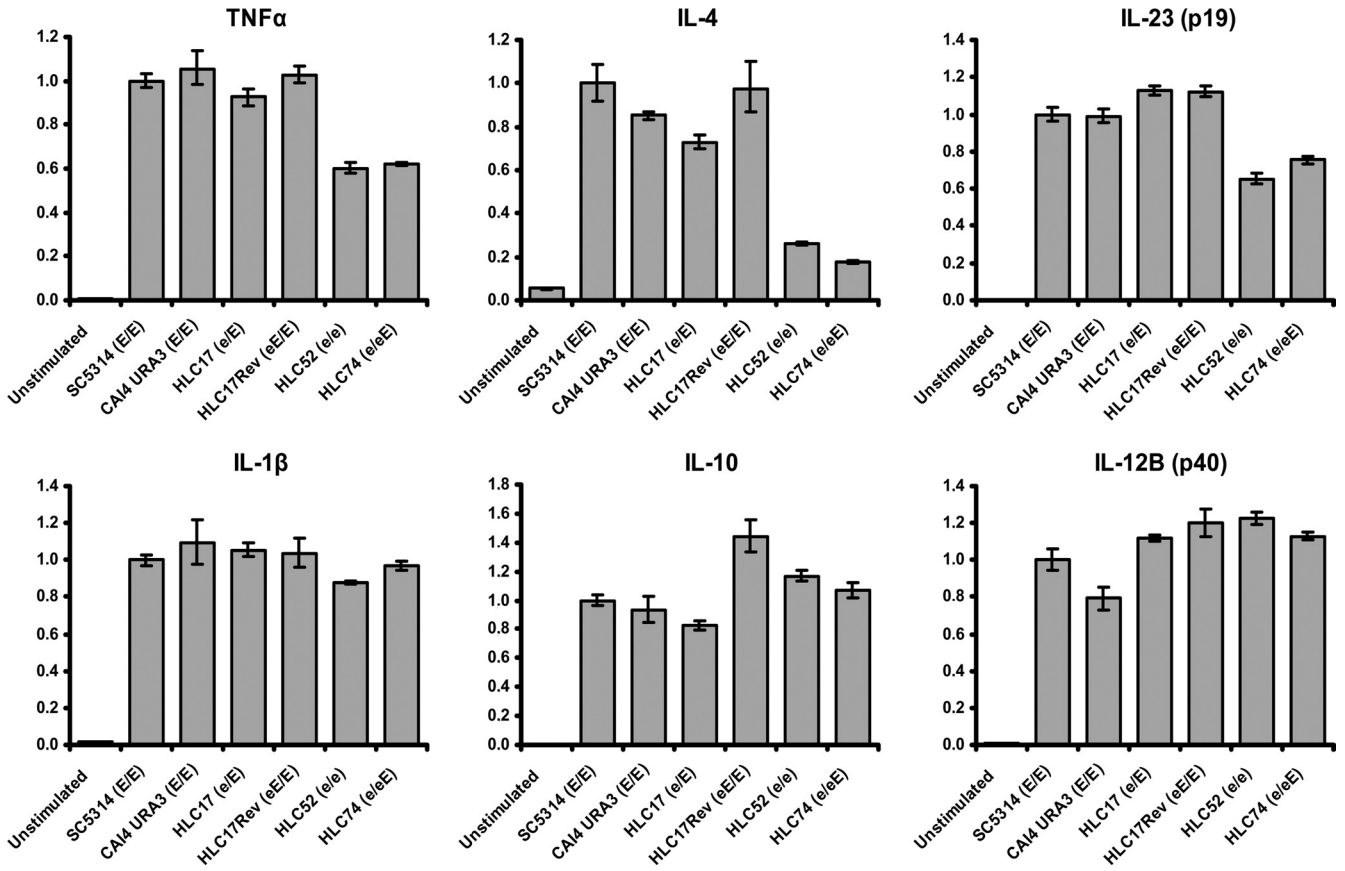

FIG 7 Transcriptional responses of unstimulated mDCs and mDCs in contact with the SC5314 wild-type, CAI4 URA3 revertant, and *EFG1* mutant strains. mRNA levels were related to the absolute level of mDCs treated with wild-type SC5314, which was set to 1. Determinations were performed in triplicate, and average values with standard deviations are presented. Results are representative of two independent experiments. In the presence of wild-type strain SC5314, the level of IL-4 was induced by 1 order of magnitude, while the rest of the studied cytokines were induced by 2 orders of magnitude, compared to the basal levels in unstimulated mDCs.

increase in ROS release in these strains due to the growth phase of the cell, like that shown for the WT, indicating that *EFG1* plays a central role in growth-phase-dependent cell wall biogenesis.

These data confirm that deletion of one *EFG1* allele in *C. albicans* already causes significant changes in its immunological properties during confrontation with macrophages. Deletion of the second *EFG1* allele pronounces this effect further. This demonstrates the importance of Efg1 for *C. albicans* cell wall biogenesis and maturation in post-exponential-phase growth. Interestingly, the higher β-1,3-glucan exposure in the *efg1/efg1* strain (HLC52) did not result in an increased ability to stimulate the ROS response, indicating that there are additional factors relevant to the ROS response in these strains. We also observed an increase in the macrophage ROS response to post-exponential-phase wild-type cells, although according to our results shown above, they expose less β-1,3-glucan in this growth phase.

Transcriptional response of mDCs to *C. albicans* deleted for *EFG1*. We performed qRT-PCR analysis to check the cytokine immune response of primary mDCs to the different *EFG1* strains (Fig. 7). As typical antigen-presenting cells, mDCs in general offer a faster and stronger response to *Candida* cells than that of macrophages. Moreover, antigen-presenting dendritic cells, usually residing on mucosal surfaces and in the skin, play important roles in anti-*Candida* protective immunity. Dendritic cells function as professional phagocytes to kill *C. albicans*, modulate the immune response, and subsequently present antigens to adaptive immune cells. In addition, defined sets of cytokines, depending on the phagocytosed pathogen, are released to direct the following immune responses. We analyzed the mRNA levels of a set of cytokines indicative of Th1, Th2, and Th17 responses in order to receive a first indication about potential changes in the immune response. Compared to the wild type, deletion of one or two copies of *EFG1* resulted in reduced expression of several cytokines, such as tumor necrosis factor alpha (TNF-α), interleukin-4 (IL-4), IL-23, and, to a minor extent, IL-1β. Reversion of both alleles (HLC17rev) resulted in WT levels or slightly higher levels. The lower cytokine response is consistent with the reduced capacity of the *efg1/efg1* null mutant to stimulate the ROS response in macrophages. In the previous experiments, we did not identify significant differences between the two strains that are heterozygous for *EFG1*, i.e., HLC17 (a heterozygote containing one WT allele at the original locus) and HLC74 (a revertant containing one *EFG1* allele expressed from the *LEU2* locus). However, the levels of TNF-α, IL-4, and IL-23 transcripts in response to HLC17 and HLC74 showed clear differences. While the HLC17 response in general resembled that of the WT, the HLC74 response resembled that of the *efg1/efg1* null mutant. This may indicate additional subtle effects due to the different chromosomal locations of *EFG1* in these strains, as also suggested by the differences in *EFG1* expression levels (Fig. 2). For additional cytokines tested (IL-10 and IL-12),

loss of *EFG1* did not result in a reduction of cytokine levels. On the other hand, when strain CAI4 URA3 was assayed, in general, no differences in expression of the studied cytokines were observed compared to the wild type. This again excludes the *URA3* gene from the observed changes in the cell wall resulting in the altered immunogenicity of the strains lacking *EFG1*. Our results indicate that the changes in cell wall structure observed previously in the *efg1/efg1* null mutant, together with changes in expression levels of genes encoding cell wall proteins, contribute significantly to its reduced immunogenic properties.

DISCUSSION

In this study, we investigated the impact of Efg1 on cell wall architecture and its ability to trigger the host response when the pathogen is in contact with immune cells.

We show that the cell wall polysaccharide structure of *C. albicans* is significantly affected by the loss of individual genomic alleles of *EFG1*. The cell wall shows a clear reduction in size, both on a morphological level and after biochemical analysis. Our results strongly suggest that this is caused by a reduction of the amount of glucan in the cell wall. This was confirmed by the increased sensitivity to both Congo red and the cell wall-degrading enzyme Zymolyase, especially in post-exponential-phase cells. This phenotype can be rationalized by previous transcriptional data showing altered regulation of genes required for cell wall biogenesis, including a subset of genes encoding cell wall synthesis and remodeling enzymes. It could also be due to a shift toward an oxidative metabolism, resulting in reduced glucose pools in the cell (9, 20, 47).

Most interestingly, *EFG1* shows severe haploinsufficiency with respect to certain cell wall-related phenotypes, indicating that the level of Efg1 is critical for proper cell surface homeostasis. Although *EFG1* haploinsufficiency is not evident for growth on Congo red, deletion of even a single *EFG1* allele impairs *C. albicans* cell wall resistance to Zymolyase. Moreover, transmission electron microscopy imaging showed a decrease in cell wall thickness after deletion of *EFG1*, which is entirely consistent with the Zymolyase hypersusceptibility. While the deletion of a single allele in both of the *efg1/EFG1* heterozygous strains reduced the average cell wall thickness by about 15%, deletion of both alleles further reduced the average cell wall thickness, to only 57% of the wild-type level. Interestingly, mannan and chitin levels seemed to be less affected than glucan levels. These data clearly indicate differences in the structures of cell walls of strains expressing Efg1 at different levels. Reintegration of a functional *EFG1* allele into a null mutant and a heterozygous strain restored the cell wall composition to heterozygote and wild-type levels, respectively, confirming Efg1 as the cause of these phenotypes. Measurements of *EFG1* mRNA levels in these strains by qRT-PCR confirmed the different expression levels of *EFG1*, as expected, but due to the low expression levels, these were more evident during post-exponential-phase growth. In general, in this growth phase, *EFG1* expression levels in HLC17rev (expressing *HA-EFG1* and the WT allele from the original locus) were increased compared to those in the WT, whereas both heterozygous strains showed reduced *EFG1* mRNA levels. No *EFG1* expression was detectable in the HLC52 deletion strain.

The reduced cell wall thickness (57%) after deletion of both *EFG1* alleles was most likely caused by smaller amounts of β-glucans present in the cell walls (only 84% of the WT level). This was observed for both exponential-phase and post-exponential-phase cells. The observed difference between the reduction in cell wall thickness (57% of the WT level) and the amount of glucan (84% of the WT level) may be due to higher densities of glucan fibers in the cell wall, which may support the stability of a weakened scaffold. An additional explanation for this may be the fact that *efg1/efg1* cells are, on average, significantly smaller in volume and thus have an altered cell surface-to-volume ratio (Table 4). The effect of *EFG1* deletion on cell morphology has already been described (28, 52). Actually, the cell size of the *efg1/efg1* null mutant is further decreased when cells go through the transition from exponential-phase to post-exponential-phase growth. As determined by FACS analysis, the mean cell size of exponential-phase and post-exponential-phase *efg1/efg1* cells decreased to 84% and 68% (Table 4) that of SC5314, respectively, decreasing the spherical surface ratio to 70% and 46%, respectively. This switch in cell size provides an additional indication for the importance of Efg1 during different growth phases.

TABLE 4 Relative cell sizes compared to exponential-phase SC5314 wild-type cells

Strain[a]	Mean cell size (±SD) relative to wild type	
	Exponential-phase growth	Post-exponential-phase growth
SC5314 (*EFG1/EFG1*)	1.00 ± 0.10	1.00 ± 0.01
CAI4 URA3 (*EFG1/EFG1*)	1.02 ± 0.24	0.92 ± 0.08
HLC17 (*efg1/EFG1*)	1.05 ± 0.03	0.79 ± 0.06
HLC17Rev (eE/*EFG1*)	1.16 ± 0.13	0.98 ± 0.04
HLC52 (*efg1/efg1*)	0.84 ± 0.10	0.68 ± 0.04
HLC74 (*efg1*/eE)	1.08 ± 0.14	1.08 ± 0.05

[a] eE, the *efg1* allele was complemented with the *EFG1* gene.

Besides the cell wall defects observed, deletion of *EFG1* strongly reduces the levels of glucose units present in intracellular oligo- and polysaccharides. This confirms for the first time, by direct biochemical evidence, the predicted metabolic changes (based on transcriptional profiling) toward increased oxidative metabolism (9). The increased oxidation of carbohydrates and the reduction of the gluconeogenesis pathway should result in reduced carbohydrate levels inside the cells.

In addition to the quantitative changes in the *C. albicans* cell wall, we also detected larger amounts of β-1,3-glucans accessible for antibody staining after deletion of *EFG1* alleles. This was the only case in which the reverted heterozygous strain (HLC17Rev) was not restored to the wild-type level but showed a similar level of β-1,3-glucan to those of the heterozygous mutants, although the quantitative glucan-to-biomass levels and macrophage responses (discussed below) between these two strains correlate. One explanation might be that the reintegrated *EFG1-HA* allele might not perfectly represent the WT situation for all aspects of Efg1 action or that the detected increase in *EFG1* mRNA in this strain may be responsible for this effect as well as for other effects observed during these studies.

Changes in β-glucan exposure often result in altered immunogenicity. Indeed, we observed significant changes in the ROS response of a murine macrophage cell line challenged with *C. albicans* strains containing different *EFG1* copy numbers. Interestingly, there appeared to be a general difference in the ROS response depending on the growth phase of *C. albicans*. For SC5314 and CAI4 URA3, a 6- to 7-fold stronger ROS response was observed in cells originating from post-exponential-phase growth, but with a slight delay, possibly indicating slower phagocytosis. This indicates that small differences in growth phase might already have a strong effect on the ROS response.

This might explain the slight differences in absolute ROS release among strains containing two *EFG1* alleles (SC5314, CAI4 URA3, and HLC17Rev). Regarding *EFG1*, exponentially growing strains deleted for either one or two *EFG1* alleles also triggered a strong ROS response, although it was delayed. For cells in post-exponential-phase growth, the ROS response of these strains dropped significantly compared to the wild type. Interestingly, the absolute ROS levels induced by these strains in exponential-phase and post-exponential-phase growth were comparable. This indicates that Efg1 is crucial for remodeling cell wall structure during different cellular growth phases. Remarkably, the macrophage ROS response did not correlate with the β-1,3-glucan exposure observed in the different strains, indicating that additional factors contribute significantly to the ROS response. This is also true for the wild type: the apparent reduced β-1,3-glucan exposure of post-exponential-phase cells in comparison to exponentially grown cells did not result in reduced ROS levels. In contrast, an induction of 6- to 7-fold was observed. However, the β-1,3-glucan stained with the antibody might not represent the β-1,3-glucan molecules detected by immune receptors of the cell, although this antibody is commonly used for discrimination of *C. albicans* strains with different levels of exposed β-1,3-glucan and linked to recognition by innate immune cells (54).

As observed for macrophages, the *C. albicans efg1/efg1* null mutant induced significantly lower expression levels of some of the signature cytokines, such as TNF-α, IL-4, and IL-23, in myeloid dendritic cells. The production of IL-4, a Th2 hallmark cytokine, has been linked to ingestion of hyphae, while production of the Th1 hallmark cytokine IL-12 is usually observed as a response to yeast-form fungal cells (10). Therefore, the reduction in IL-4 expression in mDCs ingesting the *efg1/efg1* strain may reflect its altered filamentation phenotype. The reduction of expression of TNF-α, a classical inflammatory cytokine, may be linked to changes in mannose structures of the cell wall, since TNF-α expression has been connected to stimulation of mDCs by mannoproteins (36). Furthermore, IL-23 induction in dendritic cells has been linked to β-glucan, and strains devoid of *EFG1* contain significantly less of this component (7). Additionally, we did not observe any significant reduction of the level of IL-10 or IL-12. Thus, the differences in the transcriptional response most likely were not caused by a difference in stimulus quantity (affected by cell size or amount) but rather were related to qualitative changes in polysaccharide cell wall composition. This certainly would cause different availabilities of pathogen-associated molecular patterns (PAMPs) eliciting the host immune response through the complex interplay of dedicated and PAMP-specific pattern recognition receptors (3).

The observed cell wall phenotypes of the *efg1/efg1* null mutant, in general, were not fully restored to wild-type levels by reintegration of only one functional allele of the *EFG1* gene. In accordance with this finding, the cell wall phenotypes of the initially created *efg1/EFG1* heterozygous strain were often somewhere between those of the wild type and the *efg1/efg1* null mutant. However, in most cases, the phenotypes observed for the *efg1/EFG1* heterozygous strain were restored to wild-type levels by reintroduction of a second functional *EFG1* allele. The phenotypes of the *efg1/EFG1* heterozygous strain (HLC17) and the null mutant with one restored *EFG1* allele (HLC74) were also consistent, although the functional alleles are located at different loci (the original *EFG1* locus and the *LEU2* locus, respectively). The only set of experiments where these two strains displayed partial differences was in the cytokine response of dendritic cells, but these results correlate with the *EFG1* expression patterns detected by quantitative real-time PCR. It seems that reintegration of *EFG1* into the *LEU2* locus affected its expression, potentially due to truncation of the promoter or because of a position effect of the locus. Only in this case did the *EFG1* allele position result in observable phenotypic differences.

The CAI4 URA3 strain, a *URA3* revertant of CAI4 (11), a *ura3*-deficient parent of the *EFG1*-deficient strains, did behave very similarly to the SC5314 wild-type strain with respect to cell wall stability and composition, β-1,3-glucan exposure, ROS response, and DC immune response. Previously, *URA3* expression changes due to copy number and position were described to be important for events such as hypha elongation and *in vivo* infection of mice (26, 45). However, in this case, we did not observe any significant changes in cell wall composition or immunogenicity of *C. albicans* that were dependent on *URA3*. Thus, all of the observed cell wall changes can be attributed to the *EFG1* deletion.

Taken together, our results strongly suggest that Efg1 deficiency has a severe impact on the structural components of the cell wall, in addition to the impact on cell wall protein expression reported previously (47). It is evident that loss of one *EFG1* allele in the *C. albicans* genome already leads to severe changes in cell wall homeostasis, with consequences for the immunogenicity of these strains. The reduced immunogenicity might also help to explain the slow clearance of the *efg1/efg1* mutant strain from mice after infections in a tail vein model. Additionally, the major impact of Efg1 on the cell wall might also help to explain the cell wall differences and differential virulence reported for white and opaque-phase cells, which express different Efg1 levels (1, 25, 51).

The identification of the structural changes in the cell wall caused by loss of *EFG1* reported in this work may help to explain the exceptionally attenuated virulence of *C. albicans* strains devoid of *EFG1*, together with the other phenotypes characterizing *EFG1*, including altered morphogenesis and differences in cell wall protein composition and general metabolism.

ACKNOWLEDGMENTS

We thank Michael Schweikert for kind help with transmission electron microscopy imaging, Ulrike Götz for help with HPIC measurements of carbohydrates, Theodor C. White and Nicholas Lejarcegui for help with FACS analysis, and Brooke Esquivel for proofreading. We are indebted to Ingrid Frohner for her technical advice on the ROS assays and to Joachim Ernst for the generous gift of plasmid pTD38-HA.

This work was supported by a grant for the European Marie-Curie RTN project CanTrain (MRTN-CT-2004-512481) to M.Z., S.R., and K.K. This work was also supported by a grant from the Christian Doppler Society to K.K. O.M. is a recipient of an OeAW DOCfforte Ph.D. Fellowship of the Austrian Academy of Sciences.

REFERENCES

1. **Anderson J, Mihalik R, Soll DR.** 1990. Ultrastructure and antigenicity of the unique cell wall pimple of the *Candida* opaque phenotype. J. Bacteriol. **172**:224–235.
2. **Biswas S, Van Dijck P, Datta A.** 2007. Environmental sensing and signal transduction pathways regulating morphopathogenic determinants of *Candida albicans.* Microbiol. Mol. Biol. Rev. **71**:348–376.
3. **Bourgeois C, Majer O, Frohner IE, Tierney L, Kuchler K.** 2010. Fungal attacks on mammalian hosts: pathogen elimination requires sensing and tasting. Curr. Opin. Microbiol. **13**:401–408.
4. **Care RS, Trevethick J, Binley KM, Sudbery PE.** 1999. The *MET3* promoter: a new tool for *Candida albicans* molecular genetics. Mol. Microbiol. **34**:792–798.
5. **Chamilos G, et al.** 2006. *Drosophila melanogaster* as a facile model for large-scale studies of virulence mechanisms and antifungal drug efficacy in *Candida* species. J. Infect. Dis. **193**:1014–1022.

6. **DeLeo FR, Allen LA, Apicella M, Nauseef WM.** 1999. NADPH oxidase activation and assembly during phagocytosis. J. Immunol. **163**:6732–6740.
7. **Dennehy KM, Willment JA, Williams DL, Brown GD.** 2009. Reciprocal regulation of IL-23 and IL-12 following co-activation of Dectin-1 and TLR signaling pathways. Eur. J. Immunol. **39**:1379–1386.
8. **Dieterich C, et al.** 2002. *In vitro* reconstructed human epithelia reveal contributions of *Candida albicans EFG1* and *CPH1* to adhesion and invasion. Microbiology (Reading, England) **148**:497–506.
9. **Doedt T, et al.** 2004. APSES proteins regulate morphogenesis and metabolism in *Candida albicans.* Mol. Biol. Cell **15**:3167–3180.
10. **d'Ostiani CF, et al.** 2000. Dendritic cells discriminate between yeasts and hyphae of the fungus *Candida albicans.* Implications for initiation of T helper cell immunity *in vitro* and *in vivo.* J. Exp. Med. **191**:1661–1674.
11. **Fonzi WA, Irwin MY.** 1993. Isogenic strain construction and gene mapping in *Candida albicans.* Genetics **134**:717–728.
12. **Forman HJ, Torres M.** 2002. Reactive oxygen species and cell signaling: respiratory burst in macrophage signaling. Am. J. Respir. Crit. Care Med. **166**:S4–S8.
13. **Fradin C, et al.** 2005. Granulocytes govern the transcriptional response, morphology and proliferation of *Candida albicans* in human blood. Mol. Microbiol. **56**:397–415.
14. **Francois JM.** 2006. A simple method for quantitative determination of polysaccharides in fungal cell walls. Nat. Protoc. **1**:2995–3000.
15. **Frohner IE, Bourgeois C, Yatsyk K, Majer O, Kuchler K.** 2009. *Candida albicans* cell surface superoxide dismutases degrade host-derived reactive oxygen species to escape innate immune surveillance. Mol. Microbiol. **71**:240–252.
16. **Fu Y, et al.** 2002. *Candida albicans* Als1p: an adhesin that is a downstream effector of the *EFG1* filamentation pathway. Mol. Microbiol. **44**:61–72.
17. **Gantner BN, Simmons RM, Canavera SJ, Akira S, Underhill DM.** 2003. Collaborative induction of inflammatory responses by dectin-1 and Toll-like receptor 2. J. Exp. Med. **197**:1107–1117.
18. **Gantner BN, Simmons RM, Underhill DM.** 2005. Dectin-1 mediates macrophage recognition of *Candida albicans* yeast but not filaments. EMBO J. **24**:1277–1286.
19. **Gillum AM, Tsay EY, Kirsch DR.** 1984. Isolation of the *Candida albicans* gene for orotidine-5′-phosphate decarboxylase by complementation of *S. cerevisiae ura3* and *E. coli pyrF* mutations. Mol. Gen. Genet. **198**:179–182.
20. **Harcus D, Nantel A, Marcil A, Rigby T, Whiteway M.** 2004. Transcription profiling of cyclic AMP signaling in *Candida albicans.* Mol. Biol. Cell **15**:4490–4499.
21. **Hiller E, Heine S, Brunner H, Rupp S.** 2007. *Candida albicans* Sun41p, a putative glycosidase, is involved in morphogenesis, cell wall biogenesis, and biofilm formation. Eukaryot. Cell **6**:2056–2065.
22. **Hnisz D, Majer O, Frohner IE, Komnenovic V, Kuchler K.** 2010. The Set3/Hos2 histone deacetylase complex attenuates cAMP/PKA signaling to regulate morphogenesis and virulence of *Candida albicans.* PLoS Pathog. **6**:e1000889.
23. **Jackson BE, Wilhelmus KR, Hube B.** 2007. The role of secreted aspartyl proteinases in *Candida albicans* keratitis. Invest. Ophthalmol. Vis. Sci. **48**:3559–3565.
24. **Korting HC, et al.** 2003. Reduced expression of the hyphal-independent *Candida albicans* proteinase genes *SAP1* and *SAP3* in the *efg1* mutant is associated with attenuated virulence during infection of oral epithelium. J. Med. Microbiol. **52**:623–632.
25. **Kvaal C, et al.** 1999. Misexpression of the opaque-phase-specific gene *PEP1* (*SAP1*) in the white phase of *Candida albicans* confers increased virulence in a mouse model of cutaneous infection. Infect. Immun. **67**:6652–6662.
26. **Lay J, et al.** 1998. Altered expression of selectable marker *URA3* in gene-disrupted *Candida albicans* strains complicates interpretation of virulence studies. Infect. Immun. **66**:5301–5306.
27. **Livak KJ, Schmittgen TD.** 2001. Analysis of relative gene expression data using real-time quantitative PCR and the 2(−Delta Delta C(T)) method. Methods **25**:402–408.
28. **Lo HJ, et al.** 1997. Nonfilamentous *C. albicans* mutants are avirulent. Cell **90**:939–949.
29. **Lott JA, Turner K.** 1975. Evaluation of Trinder's glucose oxidase method for measuring glucose in serum and urine. Clin. Chem. **21**:1754–1760.
30. **Lu Q, Jayatilake JA, Samaranayake LP, Jin L.** 2006. Hyphal invasion of *Candida albicans* inhibits the expression of human beta-defensins in experimental oral candidiasis. J. Invest. Dermatol. **126**:2049–2056.
31. **Nantel A, et al.** 2002. Transcription profiling of *Candida albicans* cells undergoing the yeast-to-hyphal transition. Mol. Biol. Cell **13**:3452–3465.
32. **Noffz CS, Liedschulte V, Lengeler K, Ernst JF.** 2008. Functional mapping of the *Candida albicans* Efg1 regulator. Eukaryot. Cell **7**:881–893.
33. **Park H, et al.** 2005. Role of the fungal Ras-protein kinase A pathway in governing epithelial cell interactions during oropharyngeal candidiasis. Cell. Microbiol. **7**:499–510.
34. **Phan QT, Belanger PH, Filler SG.** 2000. Role of hyphal formation in interactions of *Candida albicans* with endothelial cells. Infect. Immun. **68**:3485–3490.
35. **Phan QT, et al.** 2007. Als3 is a *Candida albicans* invasin that binds to cadherins and induces endocytosis by host cells. PLoS Biol. **5**:e64.
36. **Pietrella D, Bistoni G, Corbucci C, Perito S, Vecchiarelli A.** 2006. *Candida albicans* mannoprotein influences the biological function of dendritic cells. Cell. Microbiol. **8**:602–612.
37. **Pukkila-Worley R, Peleg AY, Tampakakis E, Mylonakis E.** 2009. *Candida albicans* hyphal formation and virulence assessed using a *Caenorhabditis elegans* infection model. Eukaryot. Cell **8**:1750–1758.
38. **Ramage G, VandeWalle K, Lopez-Ribot JL, Wickes BL.** 2002. The filamentation pathway controlled by the Efg1 regulator protein is required for normal biofilm formation and development in *Candida albicans.* FEMS Microbiol. Lett. **214**:95–100.
39. **Raschke WC, Baird S, Ralph P, Nakoinz I.** 1978. Functional macrophage cell lines transformed by Abelson leukemia virus. Cell **15**:261–267.
40. **Roncero C, Duran A.** 1985. Effect of calcofluor white and Congo red on fungal cell wall morphogenesis: *in vivo* activation of chitin polymerization. J. Bacteriol. **163**:1180–1185.
41. **Rubin-Bejerano I, Abeijon C, Magnelli P, Grisafi P, Fink GR.** 2007. Phagocytosis by human neutrophils is stimulated by a unique fungal cell wall component. Cell Host Microbe **2**:55–67.
42. **Saville SP, Thomas DP, Lopez Ribot JL.** 2006. A role for Efg1p in *Candida albicans* interactions with extracellular matrices. FEMS Microbiol. Lett. **256**:151–158.
43. **Schroppel K, et al.** 2000. Repression of hyphal proteinase expression by the mitogen-activated protein (MAP) kinase phosphatase Cpp1p of *Candida albicans* is independent of the MAP kinase Cek1p. Infect. Immun. **68**:7159–7161.
44. **Setiadi ER, Doedt T, Cottier F, Noffz C, Ernst JF.** 2006. Transcriptional response of *Candida albicans* to hypoxia: linkage of oxygen sensing and Efg1p-regulatory networks. J. Mol. Biol. **361**:399–411.
45. **Sharkey LL, Liao WL, Ghosh AK, Fonzi WA.** 2005. Flanking direct repeats of *hisG* alter *URA3* marker expression at the *HWP1* locus of *Candida albicans.* Microbiology (Reading, England) **151**:1061–1071.
46. **Sharkey LL, McNemar MD, Saporito-Irwin SM, Sypherd PS, Fonzi WA.** 1999. *HWP1* functions in the morphological development of *Candida albicans* downstream of *EFG1*, *TUP1*, and *RBF1.* J. Bacteriol. **181**:5273–5279.
47. **Sohn K, Urban C, Brunner H, Rupp S.** 2003. *EFG1* is a major regulator of cell wall dynamics in *Candida albicans* as revealed by DNA microarrays. Mol. Microbiol. **47**:89–102.
48. **Sonneborn A, Bockmuhl DP, Ernst JF.** 1999. Chlamydospore formation in *Candida albicans* requires the Efg1p morphogenetic regulator. Infect. Immun. **67**:5514–5517.
49. **Sonneborn A, et al.** 2000. Protein kinase A encoded by *TPK2* regulates dimorphism of *Candida albicans.* Mol. Microbiol. **35**:386–396.
50. **Sonneborn A, Tebarth B, Ernst JF.** 1999. Control of white-opaque phenotypic switching in *Candida albicans* by the Efg1p morphogenetic regulator. Infect. Immun. **67**:4655–4660.
51. **Srikantha T, Tsai LK, Daniels K, Soll DR.** 2000. *EFG1* null mutants of *Candida albicans* switch but cannot express the complete phenotype of white-phase budding cells. J. Bacteriol. **182**:1580–1591.
52. **Stoldt VR, Sonneborn A, Leuker CE, Ernst JF.** 1997. Efg1p, an essential regulator of morphogenesis of the human pathogen *Candida albicans*, is a member of a conserved class of bHLH proteins regulating morphogenetic processes in fungi. EMBO J. **16**:1982–1991.
53. **Weide MR, Ernst JF.** 1999. Caco-2 monolayer as a model for transepithelial migration of the fungal pathogen *Candida albicans.* Mycoses **42**(Suppl 2):61–67.
54. **Wheeler RT, Fink GR.** 2006. A drug-sensitive genetic network masks fungi from the immune system. PLoS Pathog. **2**:e35.